Turbulent Heat-Transfer Measurements on a Blunt Cone at Angle of Attack

GEORGE F. WIDHOPF*
The Aerospace Corporation, San Bernardino, Calif.

Turbulent heat-transfer rates measured on the conical surface of a blunt 9° half-angle cone in a $M_\infty = 10.6$ nitrogen flow at various angles of attack are presented. The measurements were made at a nominal Re_∞/ft of 12(10)^6 at angles of attack of $\alpha = 0°, 2.5°, 5°, 10°, 15°$, and 20°. The boundary layer was tripped in order to attain turbulent flow over the model. Detailed distributions of the heat-transfer rate and surface pressure were obtained in the circumferential ($\Delta\phi = 22.5°$) as well as the axial directions ($S/R_N \leq 10$). Turbulent heat-transfer rates computed along inviscid surface streamlines, wherein the streamline pattern was determined utilizing the experimental pressure distributions, are compared to the data. Good agreement is obtained in the regions where the assumption of neglecting the effect of entropy swallowing utilized in the analysis is valid. The turbulent heat-transfer formulation proposed by Vaglio-Laurin as being applicable in three-dimensional flows is shown to be a good approximation for these test conditions. The influence of streamline spreading is demonstrated as well as the relative accuracy of equivalent cone techniques. The results of numerical calculations of the surface pressure are compared to the data and good agreement is achieved, except in regions where viscous-inviscid interactions become important.

Nomenclature

h_2 = length element which characterizes the spreading of the streamlines
H = total enthalpy
k = roughness height (peak to valley) = 0.006 in.
l = length element along a streamline
M = Mach number
P = static pressure
Pr = Prandtl number (a value of 0.716 was used exclusively)
q = heat transfer/unit area/unit time
r = local body radius
Re = Reynolds number
R_N = nose radius
S = surface coordinate measured from $\alpha = 0°$ stagnation point
T = temperature
T_w = wall temperature (≈300°K)
U = velocity
α = angle of attack
γ = ratio of specific heats
δ_c = cone half angle
δ_T = turbulent boundary-layer thickness
μ = coefficient of viscosity
ρ = density
ϕ = circumferential angle measured from leeward ray

Subscripts

e = boundary-layer edge conditions
se = boundary-layer edge stagnation conditions
∞ = freestream
w = wall
0 = laminar stagnation-point condition, $\alpha = 0°$

Presented as Paper 71-38 at the AIAA 9th Aerospace Sciences Meeting, New York, January 25–27, 1971; submitted January 7, 1971; revision received April 23, 1971. The author wishes to acknowledge the capable assistance of J. Coble of the Arnold Research Organization Inc., in conducting the experiments and K. Reed for his efficient coding of the streamline tracing program. Thanks are also extended to F. Fernandez who originally proposed this work and to R. Eaton of Sandia Laboratories for supplying a copy of the angle-of-attack inviscid flowfield program utilized herein.

Index Category: Boundary Layers and Convective Heat Transfer—Turbulent.

* Member of the Technical Staff. Associate Member AIAA.

Introduction

IN order to ascertain the requirements necessary for the effective thermal protection of a hypersonic vehicle during re-entry, the capability of predicting surface heating rates under realistic flight conditions and attitudes must be developed and verified. Such conditions necessarily include both turbulent flow and vehicle angle of attack. The calculation of the turbulent heat-transfer rate in such a three-dimensional environment inherently involves the utilization of many simplifying assumptions in order to make the computations tactable. Verification of the acceptability of these flow models and the accuracy of the ensuing predictions invariably depends upon agreement with experimental data. To date, there is a scarcity of experimental hypersonic turbulent heat-transfer data over blunt cones at angle of attack. Thus, experimental data which depict the detailed circumferential and axial variation of the local turbulent heat transfer at angle of attack are needed. These data can then serve as a basis upon which various flow models can be evaluated as to their effectiveness in predicting the influence of the three-dimensional environment on the local turbulent heat transfer.

This paper presents the results of a test program wherein turbulent heat-transfer rates and static pressure distributions were measured on a blunt cone at various angles of attack. Numerical calculations of the turbulent heat-transfer rates are then compared to the data, as well as the results of numerical calculations of the surface pressure variation.

Experimental Facility and Test Conditions

The test program was conducted in the von Kármán Tunnel F facility at the Arnold Engineering Development Center. The measurements were made in a nitrogen environment at a freestream Mach number of approximately 10.6 and a nominal Re_∞/ft of 12(10)^6. The wall to stagnation temperature ratio (T_w/T_0) was nominally 0.3. The angles of attack considered included $\alpha = 0°, 2.5°, 5°, 10°, 15°$, and 20°.

Model Configuration and Instrumentation

The configuration utilized was a spherically capped (R_N = 2.5 in.), 9° half-angle cone. During each run, measurements

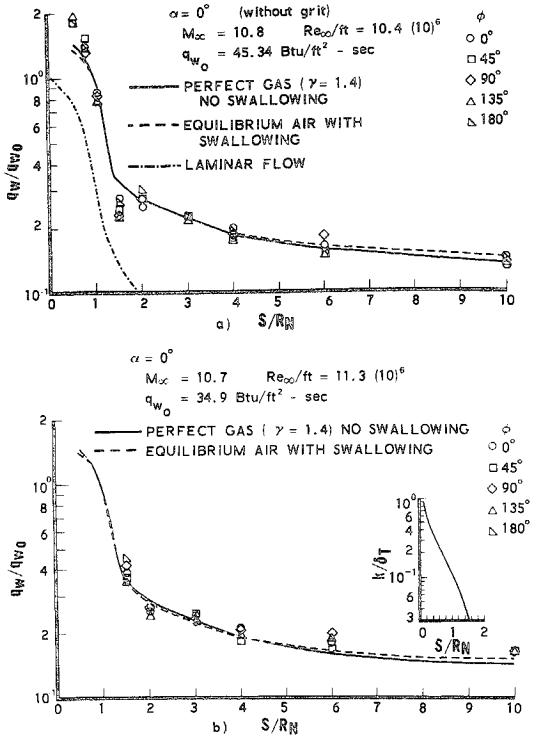

Fig. 1 Comparison between calculated and experimental turbulent heat-transfer distribution at $\alpha = 0°$.

of either the static pressure or the heat-transfer rate were made at nine stations (S/R_N = 0.52, 0.79, 1.05, 1.5, 2, 3, 4, 6, and 10) along five axial rays, spaced every 45° in the circumferential direction.

The hemispherical portion of the model was roughened in order to insure the attainment of turbulent flow over this region. The roughness consisted of 0.006-in. silica carbide grit which was adhered to the surface utilizing a thin layer of adhesive. The grit configuration consisted of a relatively low-density spatial arrangement of randomly oriented and distributed roughness elements. It was necessary to extend the roughness region up to $S/R_N = 1.45$ since, under the present test conditions, the flow tended to "laminariarize"[1] around the shoulder region. The effect of this phenomenon on the local heat-transfer rate is shown in Fig. 1a for the zero angle-of-attack case. These measurements were made on a model on which no roughness elements were applied. The drop (approximately 35%) in heat-transfer rate near the shoulder is due to the "laminarizing" of the flow which results from the high flow acceleration around the hemispherical portion of the model. Shown in Fig. 1b is the heat-transfer rate measured on a model roughened in the manner previously described. Here it is noticed that the heat-transfer rate no longer exhibits this drop, and the turbulent heat-transfer rate now agrees with the theoretical value. (These comparisons will be discussed further later on.) The laminar heat-transfer distribution is included in order to give a better perspective of the relative effect of "laminarization" on the local heat-transfer rate. Also shown is the variation of the roughness height to the local turbulent boundary-layer thickness.

Tests conducted at $\alpha = 10°$, wherein the axial extent of the grit was varied, showed that, within the experimental accuracy, only the "laminarization" regions were affected. They also demonstrated the necessity of extending the grit up to the shoulder in order to avoid any "laminarization" of the flow. Tests conducted at $\alpha = 0°$ demonstrated that all grit sizes in the range of 0.003–0.011 in. affected the flow in a similar manner; that is, they effectively served as a means whereby the existence of turbulent flow is insured even in the regions where "laminarization" previously occurred. Thus,

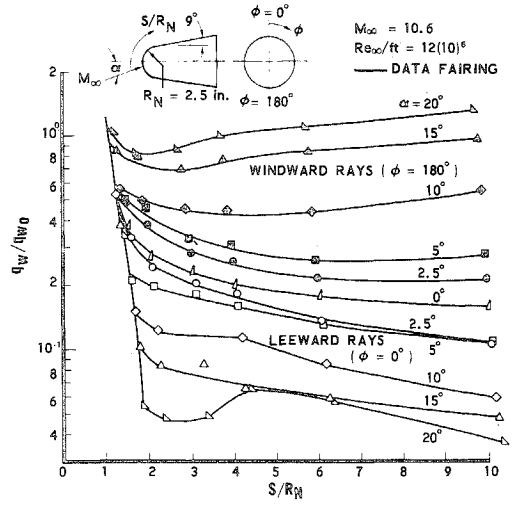

Fig. 2 Turbulent heat-transfer distributions along the windward and leeward rays for various angles of attack.

all of these tests indicate that, within the given experimental error, the grit effectively served as a local source of disturbance, sustaining the turbulent flow until it passed the region of high acceleration ("laminarization" region), while not affecting the downstream heat-transfer values. The localized effect of roughness on the heat-transfer rate was also observed in Ref. 2. The heat-transfer rates which were measured on the smooth conical portion of the model are presented in this paper.

The heat-transfer measurements were made utilizing a fast-response, calorimeter-type, heat-transfer gage which utilizes a sputtered thin film platinum resistance thermometer to sense the temperature rise of the gage backface.[3,4] The accuracy of the resulting measurements is estimated to be ±10% over most of the range of the measurements. The pressure measurements were made utilizing fast-response differential strain gage and variable reluctance transducers.[3,4] The accuracy of these measurements is estimated to be ±5% for most of the data, but somewhat larger (±10%) at the very low pressures.

Procedure

Separate runs were made to obtain the heat-transfer and static pressure data. For each angle of attack, excluding $\alpha = 20°$, the model was rolled $\phi = -22.5°$, yielding an effec-

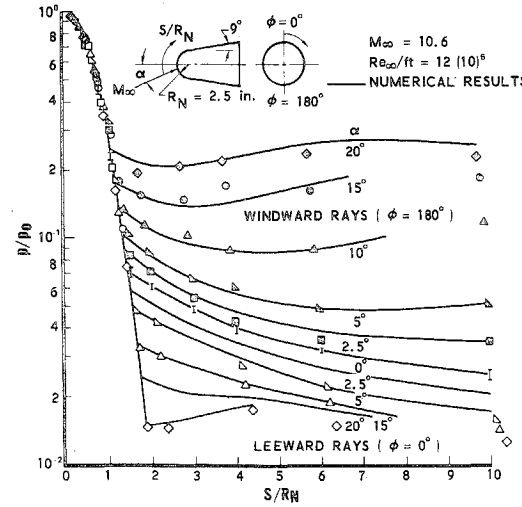

Fig. 3 Surface pressure distributions along the windward and leeward rays for various angles of attack.

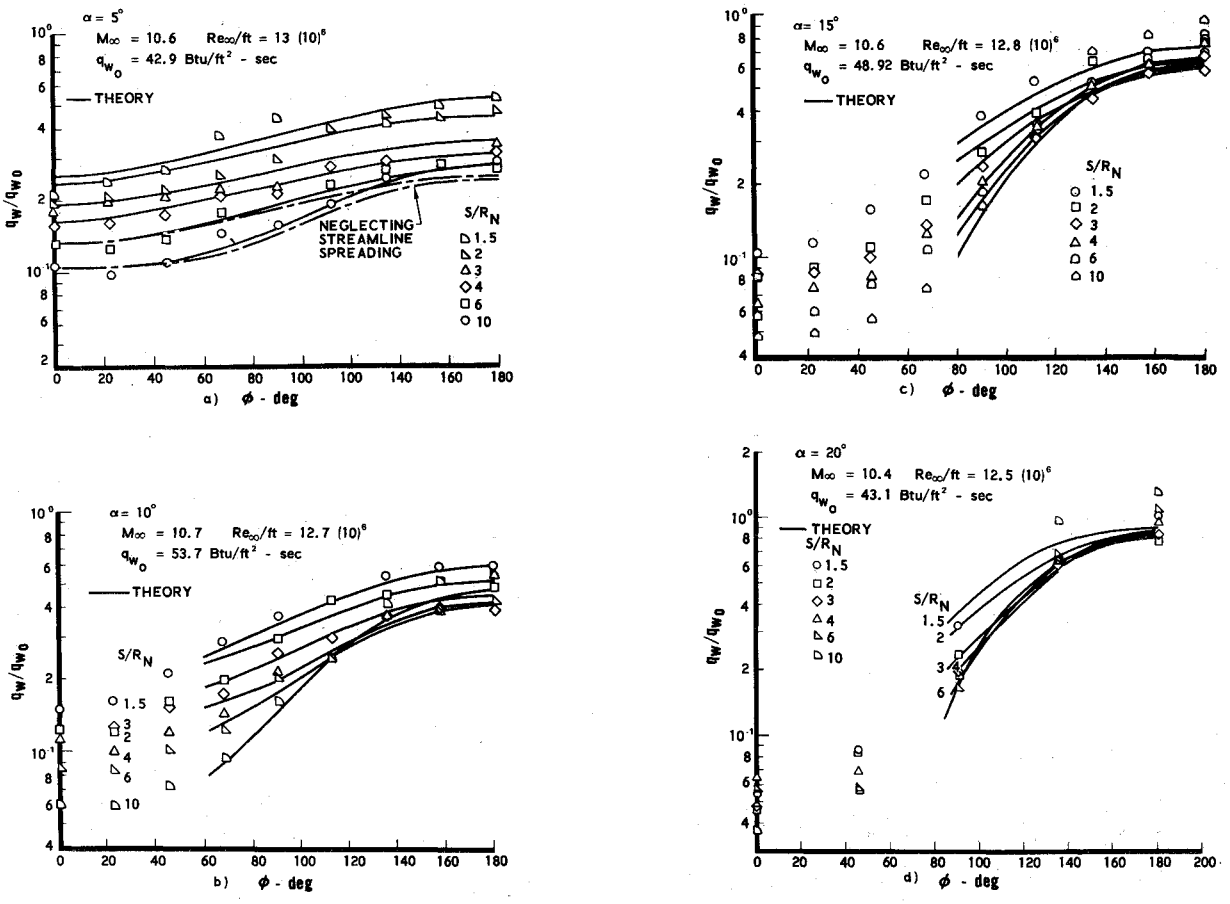

Fig. 4 Comparison between the calculated and experimental circumferential turbulent heat-transfer distributions at various axial stations.

tive circumferential distribution every 22.5°. Thus, detailed distributions of the heat-transfer rate were obtained both in the axial and circumferential directions. In subsequent tests, all the gages were replaced with pressure transducers and the same procedure was repeated, excluding roll runs for α = 2.5° and 20°.

During each run, separate measurements of the laminar stagnation heat-transfer rate were made on hemisphere-cylinders arranged in an $\alpha = 0°$ configuration, together with measurements of the tunnel reservoir and pitot pressures. These measurements were utilized to determine the tunnel freestream conditions (see Ref. 5) and were also used to nondimensionalize the data for each run. The stagnation heat-transfer rate measurements were scaled in order to obtain the proper nondimensionalization factor appropriate for the given test model geometry.

It should be mentioned that the freestream conditions are determined utilizing the stagnation conditions measured previously in conjunction with the theory of Fay and Riddel.[6] Thus, for the experimental conditions reported herein, the stagnation heat-transfer rate measurements listed in the legend of each figure agree with this theory.

Experimental Results

The nondimensional heat-transfer rate distributions along the windward and leeward rays at various angles of attack are depicted in Fig. 2. Here, as in every figure, the local heat-transfer rates have been nondimensionalized in the manner previously described. In this figure, the surface coordinate is measured in an angle-of-attack coordinate system as indicated. At the higher angles of attack, the heating along the windward ray is approximately equal to the laminar stagnation rate along the entire vehicle length. Thus, turbulent heating rates can become very high even at moderate angles of attack. Also, the heating rates on the windward and leeward rays can differ by more than an order of magnitude. The ability to reproduce these results serves as a rigorous test of the capabilities of various prediction methods.

Shown in Fig. 3 are the corresponding surface pressure distributions. Here, theoretical distributions calculated utilizing the computer program described in Ref. 7 have been superimposed on the data. These comparisons will be discussed later on. The similarity in contour of these two distributions is a noteworthy aspect of these figures, indicating that, under these experimental conditions, the heat-transfer rate distributions follow the pressure contours rather closely for all the angles of attack considered.

Circumferential distributions of the heat-transfer rate for α = 5°, 10°, 15°, and 20° are shown in Figs. 4a–4d. No unusual features are discernible and, in all cases, the heat-transfer rate decreases rather smoothly from its maximum at the windward ray to its value on the leeward ray. Shown in Figs. 5a–5c are the nondimensional pressure data for some typical angles of attack plotted in a manner similar to the heat-transfer data.† Examination of these distributions indicates that, at the higher angles of attack, the circumferential pressure has a minimum at a location other than at the leeward ray. This is an indication that, in these cases, flow separation can be expected to occur near the leeward region of the cone. Except for these regions, it is noticed that the heat-transfer and the pressure distributions are similar in shape and contour.

In Fig. 6, the circumferential heat-transfer distributions at one S/R_N station are crossplotted for all the angles of attack. Here, it is interesting to note that the heat transfer at the 90° meridian is approximately equal (within ±10%) to the α =

† A complete set of figures as well as tabulations of the data are included in Ref. 8.

0° value for all angles of attack up to $\alpha = 15°$. This is also true for all of the other stations, as can be seen in Fig. 7. Included in this figure are the corresponding pressure distributions where the same behavior is evident. This behavior was also observed in the laminar case as described in Ref. 9. This would imply that, along this meridian, entropy swallowing and streamline spreading are not very important in the determination of the local heat-transfer rate. This indication will be borne out later when the results of various numerical predictions are compared to the data.

When the heat-transfer rates along the windward and leeward rays were plotted on semilog scale as a function of angle of attack for each station, the heat-transfer variation for $\alpha \leq 15°$ was found to be approximated, within experimental error, by a straight line.[8] This is also true for all the other circumferential rays and simplifies interpolations to any inclusive angle of attack.

Comparison with Numerical Results

Heat-Transfer Rate Distributions

Turbulent heat-transfer rates computed along inviscid surface streamlines traced on the conical surface of a blunt cone at angle of attack were compared to the data. The turbulent heat-transfer formulation proposed by Vaglio-Laurin[10] for three-dimensional flows was utilized to compute the rates along each streamline. This relation was derived for the case of a highly cooled wall in the presence of a moderate external Mach number. Under these conditions it was shown[10] that the crossflow and the pertaining Reynolds stresses in a general three-dimensional turbulent boundary layer are negligible even for large transverse pressure gradients. Vaglio-Laurin[10] also showed that the applicability of this relation may extend to a moderately cooled wall ($T_w/T_0 = 0.5$) as well. Thus, this relation should be applicable under the present test conditions.

The heat-transfer relation is of the form

$$q_w = 0.029 Pr^{-2/3}(H_e - H_w)\rho_e U_e \mu_e h_2^{1/4} \mu_{se}^{-3/5} \cdot \left\{\int_0^l \rho_e U_e \mu_e h_2^{5/4} dl\right\}^{-1/5} \text{power} \quad (1)$$

wherein the reference conditions have been chosen to be the boundary-layer edge stagnation properties. An objective of this paper is to determine the applicability of this formulation in a three-dimensional environment, since previous comparisons were limited to axisymmetric conditions.[10]

The streamline pattern was determined utilizing the experimental pressure distributions wherein the calculation of the streamline direction and the metric h_2, which characterizes the spreading of the streamlines, is the same as that described in Refs. 11 and 12. In each case, the streamline tracing was initiated at the shoulder of the model where these initial conditions were obtained by integrating along axial rays from the most forward point of the model to the shoulder. The perfect gas ($\gamma = 1.4$) boundary-layer edge conditions were computed utilizing the given experimental surface pressure distribution in conjunction with the assumption that the boundary-layer edge properties could be characterized by the normal shock entropy. This inherently assumed that the boundary layer was negligibly thin. Thus, the phenomenon of entropy swallowing, which can become important in rotational flows, was not considered. Its conclusion is not a trival task and, thus, the determination of the turbulent heat-transfer rates excluding this effect is a logical first step. Since the region considered in these experiments (i.e., $S/R_N \leq 10$) is still more or less dominated by the flow passing through the strong shock region, this assumption should be appropriate over a large portion of the surface. Areas of disagreement between the data and theory should, therefore, elucidate the regions where entropy swallowing may be of importance.

Comparisons between the calculated and experimental circumferential and axial distributions are shown in Figs. 4a–4e and 8a–8e, respectively, for each angle of attack. In each of these computations, the experimental conditions were utilized. Here, the calculated values of the turbulent heat-transfer rate

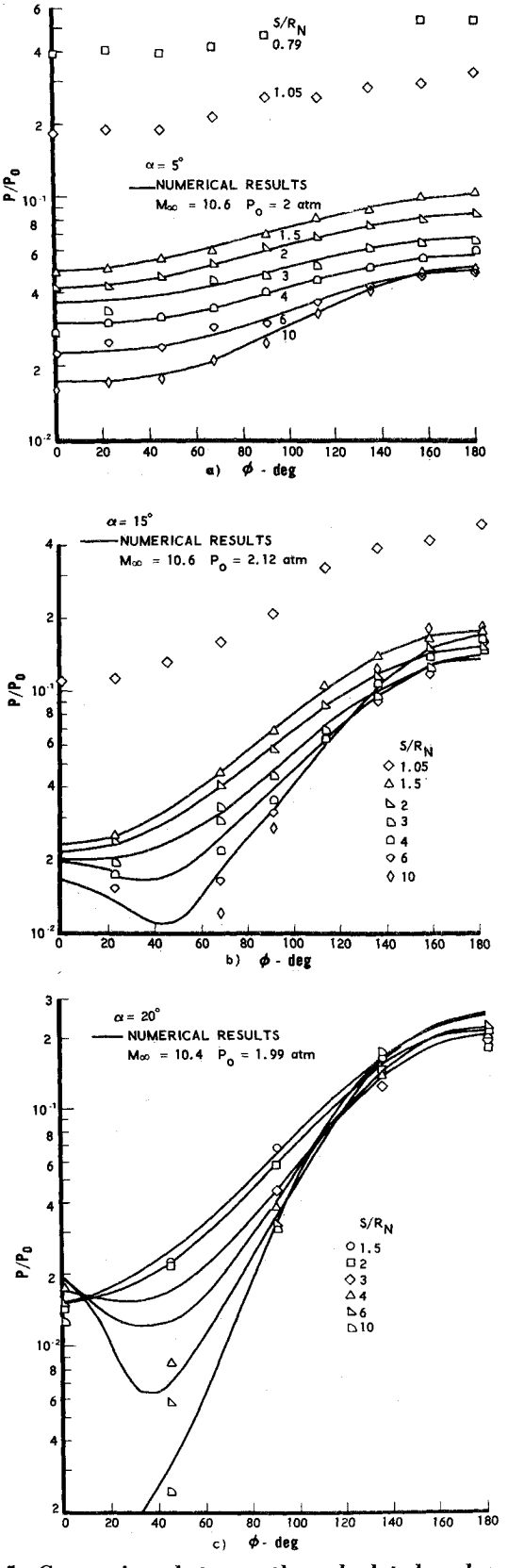

Fig. 5 Comparison between the calculated and experimental circumferential surface pressure distributions at various axial stations.

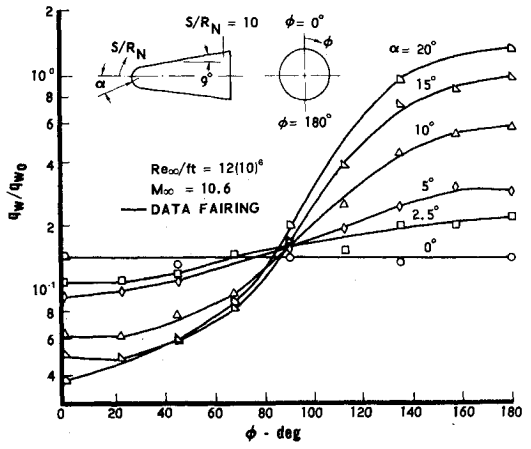

Fig. 6 Variation of the circumferential turbulent heat-transfer rate with angle of attack at axial station S/R_N = 10.

have also been nondimensionalized with respect to the experimental laminar stagnation rate, thereby allowing, in a convenient form, a direct comparison between absolute rates.

Initially, some rather general statements can be made about these comparisons. As can be seen from the figures, the numerical results and experimental data are in fairly good agreement (approximately ±15%) from the windward ray to the 90° meridian for all angles of attack. In this range, marked differences occur only at the far downstream locations for the larger angles of attack. Predictions beyond the 90° meridian are in good agreement only for the smaller angles of attack (α = 2.5° and α = 5°) as can be seen in Figs. 8a and 4b. Individual exceptions to these statements can be noted in each case and are usually the result of some scatter in the data, as can be noticed for α = 2.5°, or the apparent slight "laminarization" near the leeward shoulder for α = 5°.

Shown in Fig. 9 are the corresponding streamline directions for the cases discussed previously as computed utilizing the analysis previously described. Selected streamlines have been depicted in order to illustrate the variation in streamline divergence with angle of attack. These traces should be viewed as depicting the relative divergence rather than the absolute streamline directions because of the approximations involved in their calculation.

Entropy Swallowing

Numerical results for the α = 0° cases were obtained utilizing the perfect gas formulation previously described and also by computing the boundary-layer properties (assuming an equilibrium air gas model) including the effect of entropy swallowing.[13] In each of these computations, Eq. (1) was utilized to compute the heat-transfer rate. The results for models with and without roughness elements on the forward portion of the model are depicted in Figs. 1a and 1b, respectively. The equilibrium air predictions have been nondimensionalized with respect to the computed value of the laminar stagnation rate (utilizing the Fay and Riddell formulation) in order to minimize the effect of using equilibrium air properties in the calculations. For both of these calculations, the pressure distribution computed by the swallowing program (Ref. 13) was used in order to directly assess the effect of including entropy swallowing. This pressure distribution agrees with the experimental distribution. From these figures, it is seen that the effect of entropy swallowing only becomes apparent (for α = 0°) at the far downstream locations (i.e., $S/R_N \leq 5$). The difference in the predicted rates is approximately 10% at the most downstream location and demonstrates the improvement in the numerical results when entropy swallowing is included. In general, the agreement between the numerical calculations and the data is good.

Thus, the inclusion of entropy swallowing (thereby improving the calculation of the local flow properties) is seen to improve the accuracy of the numerical predictions for α = 0°. Analogous improvements in the angle-of-attack computations would also be expected, since the areas of major disagreement present in these cases encompass the regions where entropy swallowing is expected to be of most importance. An examination of the structure of the shock layer enveloping a blunt cone at moderate angle of attack is helpful in reinforcing these ideas. Inviscid shock layer calculations performed utilizing the computer program described in Ref. 7 show the existence of large normal entropy gradients on the windward side and substantial circumferential variations at the larger angles of attack. Since the boundary-layer thickness on the leeward side can be fairly large, the representation of the edge conditions by normal shock entropy considerations is not always a good approximation. Even on the windward side, the boundary layer will eventually ingest that mass flow which passes through the strong shock region and, again, the representation fails somewhere downstream. Since the effect of the streamline spreading is minimal on the leeward side (as is shown in Fig. 9 and to be subsequently amplified), the implication is that the influence of entropy swallowing is the important phenomenon (other than separation) to be concerned with in this region.

Streamline Spreading

In order to determine the effect of completely neglecting the streamline spreading, calculations of the turbulent heat transfer were made along conical rays (thus, the streamlines were no longer traced) utilizing the local body radius in place of the streamline metric h_2. A comparison between these and the previous results gives an indication of the magnitude of the effect of the streamline spreading on the turbulent heat-transfer rates over its range of influence. Some indicative results are shown in Figs. 8a–8e. Here, it is seen that the main differences (a maximum of approximately 30% for these conditions) occur on the more windward rays and are already minimal at the 90° meridian.

In general, the effect of neglecting the streamline divergence is seen to increase in the downstream direction and also with increasing angle of attack. Thus, the inclusion of this effect is necessary in the general case, although its exclusion can be justified in some regions as is indicated by the previous comparisons. It should be remarked that the effect of streamline

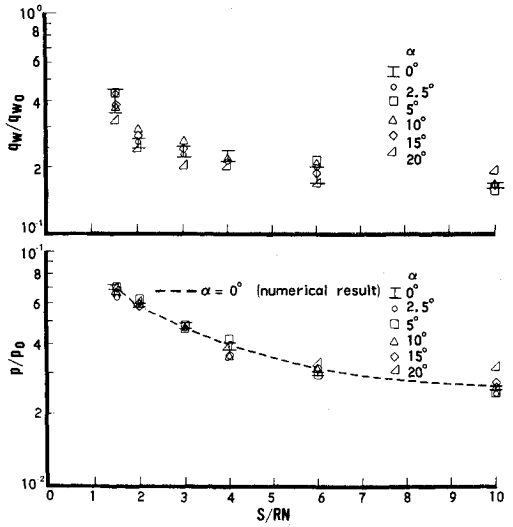

Fig. 7 Heat transfer and pressure distributions along the ϕ = 90° ray for various angles of attack.

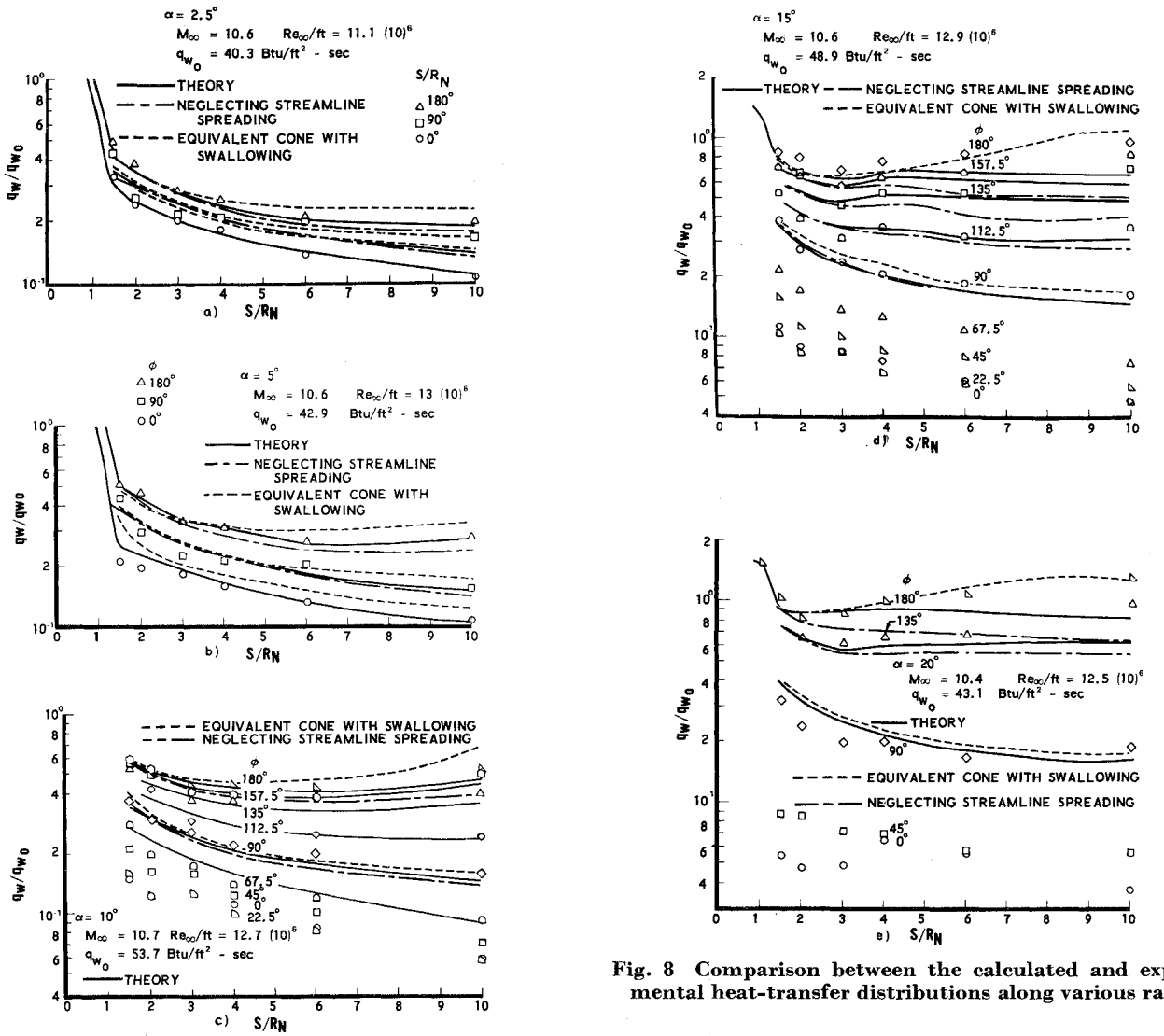

Fig. 8 Comparison between the calculated and experimental heat-transfer distributions along various rays.

spreading on the local heat-transfer rate is more pronounced when the flow is laminar.

There are more sophisticated approaches[14,15] to determine the local streamline directions and the spreading factor h_2, but the approximate method utilized herein seems to suffice in view of the fact that the influence of the streamline spreading on the local turbulent heat rate is not that significant. This conclusion is also substantiated by the acceptable agreement shown in Ref. 11 for the laminar case, where the spreading effect on the heat-transfer rate is more pronounced. The important factor in any of these computations is a correct representation of the pressure field since this is the controlling factor.

Equivalent Cone

Calculations were made to determine the degree of accuracy involved in applying the equivalent cone approximation to predict the heat-transfer rates. Computations for the windward, 90° and leeward rays, as applicable, where made utilizing the equilibrium air program (including swallowing) mentioned previously. The results of the comparisons are indicated in Figs. 8a–8e. In general, the distribution calculated for the $\phi = 90°$ ray agreed with the streamline tracing calculations, while the predictions for the leeward ray were not in good agreement (approximately 25%). The results for the 90° ray were expected due to the behavior of the pressure and heat transfer along this ray as discussed previously. Distributions for the windward ray were in fair agreement. For the larger angles of attack, these estimates (along the windward ward, ray) agree more closely with the data than the streamline calculations. This is somewhat fortuitous, since the demonstrated important influence of streamline spreading was neglected therein, while entropy swallowing was included. It must be remembered that, even in this case, the entropy swallowing was not properly accounted for since, in an equivalent cone approximation, the swallowing process does not necessarily approximate that which actually occurs in the three-dimensional case. Thus, the mixture of assumptions involved in this approximation fortuitiously resulted in a good estimate in some cases. Multiplication of these distributions by 0.91 will yield distributions nondimensionalized with respect to the computed equilibrium air stagnation rate instead of the measured rate. This was done in the zero angle-of-attack case in order to eliminate possible errors introduced by using an equilibrium air model to calculate the local flow properties.

Pressure Distributions

Surface pressure distributions were calculated for the angles of attack considered utilizing the computer program described in Ref. 7. This program calculates the inviscid flowfield surrounding a blunt cone at angle of attack. The static pressure distributions computed in this manner were compared to the measurements, the results of which have been shown in Figs. 2 and 5a–5c.

The agreement is very good for all the angles of attack except $\alpha = 20°$. In general, the distributions for $\alpha = 5°$, 10°,[8] and 15° show good agreement with the data, even adequately predicting the occurrence of pressure minimums off of the lee-

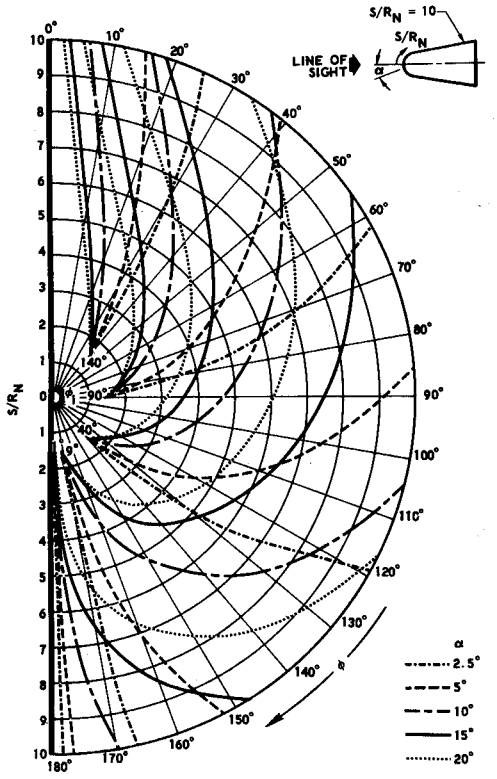

Fig. 9 Streamline traces for various angles of attack.

ward ray. For the larger angles of attack, the agreement breaks down in regions where it is evident that the effect of viscous-inviscid interactions should become important (see Figs. 5a–5c). These comparisons (Fig. 3) indicate that source flow effects arising due to the conical nozzle of the tunnel seem to be minimal.

Examination of the downstream circumferential pressure distributions implies that flow separation would occur because of the existence of adverse circumferential pressure gradients. This, in conjunction with the appearance of longitudinal vortices, presents conceptual difficulties in formulating a simple method of predicting the heat transfer on the leeward side of blunt cones when the angle of attack is larger than the cone half angle.

Conclusions

The results of this investigation may be summarized by the following: 1) Predictions utilizing Vaglio-Laurin's heat-transfer formulation are in good agreement with the data in regions where the flow model utilized is valid. From these comparisons, this formulation seems to be a good approximation which can be used to calculate turbulent heat-transfer rates over blunt cones at angle of attack. 2) Numerical calculations of the surface pressure distribution agree with the data except in regions where viscous-inviscid interactions become important. 3) Windward heating rates can approximate the laminar stagnation rate along the entire vehicle length for moderate angles of attack ($\alpha/\delta_c \approx 2$). 4) The heat-transfer rate and pressure distribution along the $\phi = 90°$ ray are practically independent of angle of attack for $\alpha/\delta_c < 2$. 5) Turbulent heat-transfer rates at moderate angles of attack ($\alpha/\delta_c \approx 2$) can vary by more than an order of magnitude from the windward to leeward rays. 6) The pressure and heat-transfer distributions have the same contours except on the leeward side at large angles of attack. 7) For the configuration and angles of attack considered, the influence of streamline spreading is confined to the windward side. 8) Equivalent cone techniques do not yield uniformly valid approximations but may provide acceptable results in some cases.

The observations outlined herein are, of course, limited in the strict sense to the angles of attack and conditions considered herein but, where indicated, can be extended to more general situations. For larger values of α/δ_c, the range of influence of the streamline spreading and entropy swallowing on turbulent heat-transfer rates would be extended. In general, both entropy swallowing and streamline spreading must be included in any analysis in order to obtain uniformly valid estimates of the turbulent heat-transfer rates. This, of course, could have been stated initially (but without the benefit of some useful qualifying statements and results) by drawing from previous examples of the importance of these phenomena, but these comparisons are helpful in defining the order of magnitude and range of influence of these phenomena.

References

[1] Sternberg, J., "Transition from a Turbulent to a Laminar Boundary Layer," Rept. 906, May 1954, Ballistic Research Labs., Aberdeen, Md.

[2] Otis, J. H., Jr., et al., "Strategic Reentry Technology Program (STREET-A)," Final Rept., Vol. II, AVSD-0210-70-RR, Vol. II, SAMSO TR-70-247, Vol. II, Nov. 1970, Avco Systems Div., Wilmington, Mass.

[3] Ledford, R. L., Smotherman, W. E., and Kidd, C. T., "Recent Developments in Heat Transfer Rate, Pressure and Force Measurements for Hotshot Tunnels," *Proceedings of the 2nd International Congress on Instrumentation in Aerospace Simulation Facilities*, IEEE, Aug. 1966.

[4] Bynum, D. S., "Instrumentation for the AEDC/VKF 100-inch Hotshot Tunnel F," AEDC-TR-66-209, Jan. 1967, ARO Inc., Arnold Engineering Development Center, Tullahoma, Tenn.

[5] Grabau, M., Smithson, H. K., Jr., and Little, W., "A Data Reduction Program for Hotshot Tunnels Based on the Fay-Riddell Heat Transfer Rate Using Nitrogen at Stagnation Temperatures from 1500° to 5000°K," AEDC TDR-64-50, June 1964, ARO Inc., Arnold Engineering Development Center, Tullahoma, Tenn.

[6] Fay, J. A. and Riddell, F. R., "Theory of Stagnation Point Heat Transfer in Dissociated Air," *Journal of the Aeronautical Sciences*, Vol. 25, No. 2, Feb. 1958, pp. 73–85.

[7] Abbett, M. J. and Fort, R., "Three-Dimensional Inviscid Flow about Supersonic Blunt Cones at Angles of Attack, III: Coupled Subsonic and Supersonic Programs for Inviscid Three-Dimensional Flow," Sandia Labs. SC-CR-68-3728, Sept. 1968, General Applied Science Lab., Westbury, N.Y.

[8] Widhopf, G. F., "Turbulent Heat Transfer Measurements on a Blunt Cone at Angle of Attack," TR-0059(S6816-66)-1, Feb. 1971, The Aerospace Corp., San Bernardino, Calif.

[9] Zakkay, V., "Pressure and Laminar Heat Transfer Results in Three-Dimensional Hypersonic Flow," WADC TN 58-182, Sept. 1958, Polytechnic Institute of Brooklyn, Farmingdale, N.Y.

[10] Vaglio-Laurin, R., "Turbulent Heat Transfer on Blunt-Nosed Bodies in Two-Dimensional and General Three-Dimensional Hypersonic Flow," *Journal of the Aerospace Sciences*, Vol. 27, No. 1, Jan. 1960, pp. 27–36.

[11] Sanlorenzo, E. A., "Method for Prediction of Streamlines and Heat Transfer to Bodies in Hypersonic Flow," GASL TR No. 177, July 1960, General Applied Science Lab., Westbury, N.Y.; also "Method for Calculating Surface Streamlines and Laminar Heat Transfer to Blunted Cones at Angle of Attack," *Journal of the Aerospace Sciences*, Vol. 28, No. 11, Nov. 1961, pp. 904–905.

[12] Vasiliu, J., "Calculation of Surface Streamlines and Laminar Heat Transfer Rates for Blunt Cones in Three-Dimensional Flow," ATM-66(6560)-11, July 1965, Aerospace Corp., San Bernardino, Calif.

[13] Jacobs, H. R., "Engineering Approximation of the Effects of Blunting on Cones in Laminar and Turbulent Flow," TR-0158-(S3816-41)-1, Oct. 1967, Aerospace Corp., San Bernardino, Calif.

[14] Vaglio-Laurin, R., "Laminar Heat Transfer on Three-Dimensional Blunt Nosed Bodies in Hypersonic Flow," *ARS Journal*, Vol. 29, No. 2, Feb. 1959, pp. 123–129.

[15] Harris, E. L., "Determination of the Streamlines on a Sphere-Cone at Angle of Attack from the Measured Surface Pressure Distribution," NOLTR 63-97, Feb. 1963, U.S. Naval Ordnance Labs., Silver Spring, Md.